

On discrete FitzHugh–Nagumo reaction–diffusion model: Stability and simulations

Iqbal M. Batiha^{a,b,*}, Osama Ogilat^c, Amel Hioual^d, Adel Ouannas^d, Nidal Anakira^{e,f}, Ala Ali Amourah^{e,g}, Shaher Momani^{b,h}

^a Department of Mathematics, Al Zaytoonah University, Amman 11733, Jordan

^b Nonlinear Dynamics Research Center (NDRC), Ajman University, Ajman, UAE

^c Department of Basic Sciences, Faculty of Arts and Science, Al-Ahliyya Amman University, Amman 19111, Jordan

^d Department of Mathematics and Computer Science, University of Oum EL-Bouaghi, Oum El Bouaghi 04000, Algeria

^e Faculty of Education and Arts, Sohar University, Sohar 3111, Oman

^f Applied Science Research Center, Applied Science Private University, Amman 11937, Jordan

^g Jadara Research Center, Jadara University, Irbid 21110, Jordan

^h Department of Mathematics, Faculty of Science, University of Jordan, Amman 11942, Jordan

ARTICLE INFO

Keywords:

FitzHugh–Nagumo reaction–diffusion system

2nd-difference approximation

L1-difference approximation

Direct Lyapunov method

ABSTRACT

This research paper focuses on the analysis of a discrete FitzHugh–Nagumo reaction–diffusion system. We begin by discretizing the FitzHugh–Nagumo reaction–diffusion model using the second-order and L1-difference approximations. Our study examines the local stability of the equilibrium points of the system. To identify conditions that ensure the global asymptotic stability of the steady-state solution, we employ various techniques, with a primary focus on the direct Lyapunov method. Theoretical results are supported by numerical simulations that demonstrate the practical validity of the asymptotic stability conclusions. Our findings provide new insights into the stability characteristics of discrete FitzHugh–Nagumo reaction–diffusion systems and contribute to the broader understanding of such systems in mathematical biology.

1. Introduction

With the aim of simplifying the Hodgkin–Huxley model, certain local dynamics were employed by FitzHugh and Nagumo et al.^{1,2} There are four ordinary differential equations (ODEs) that forms the Hodgkin–Huxley model, which were established to identify the potential's change in the giant axon of the squid across the membrane of a nerve cell.^{3–7} The FitzHugh–Nagumo (FHN) system, which comprises of two partial differential equations (PDEs), can be yielded by reducing the Hodgkin–Huxley model. For a long period of time, many implementations have employed this kind of equations, see Refs. 3, 8–20. For instance, the FHN system can be employed to describe the reentry analysis within heart tissue,²¹ Medaka eggs,⁴ the Ca^{+2} waves on *Xenopus* oocytes,³ and the C O oxidation on *Pt(110)*.cite3 For further implementations of this system and its relevance for the discretization, the reader may refer to the Refs. 22–29.

Many researchers have recently carried out numerous studies for addressing the analysis of the FHN reaction–diffusion model. For instance, with the use of the nonstandard finite difference approach, a numerical approximation of the FHN model was proposed in Ref. 30.

For the Nagumo equation, a boundedness preserving finite volume approach was established in Ref. 31. In the same regard, several methods were also used to deal with the conventional FHN equation that were formulated in accordance with certain boundary and initial conditions.³² The FHN model in terms of its positivity and boundedness was also handled in Ref. 33 with the aid of four nonstandard versions of finite difference methods under three different regimes and according to certain boundary and initial conditions. Furthermore, the Newell–Whitehead and FHN models were addressed in Ref. 34, and then a novel improvement of the finite difference approach in its explicit exponential version with its analytical scheme were consequently discussed in the same reference. More recently, the FHN reaction–diffusion model was approximated by means of applying the piecewise-linear finite element method for the purpose of describing the action potentials' propagation in the cells of cardiac muscle.³⁵

A great deal of investigations has convincingly outlined the FHN reaction–diffusion model, but these investigations do not incorporate an attentive analytical examination for the discrete type of such a

* Corresponding author at: Department of Mathematics, Al Zaytoonah University, Amman 11733, Jordan.

E-mail addresses: i.batiha@zuj.edu.jo (I.M. Batiha), o.ogilat@ammanu.edu.jo (O. Ogilat), amel.hioual@univ-oeb.dz (A. Hioual), ouannas.adel@univ-oeb.dz (A. Ouannas), nanakira@su.edu.om (N. Anakira), s.momani@ju.edu.jo (S. Momani).

<https://doi.org/10.1016/j.padiff.2024.100870>

Received 3 June 2024; Received in revised form 31 July 2024; Accepted 11 August 2024

Available online 13 August 2024

2666-8181/© 2024 The Author(s). Published by Elsevier B.V. This is an open access article under the CC BY-NC-ND license (<http://creativecommons.org/licenses/by-nc-nd/4.0/>).

model with studying its stability. For this reason, the primary objective of this research paper is to analyze the discrete FHN reaction–diffusion system. In this connection, the 2nd- and $L1$ -difference approximations will be utilized to first discretize the FHN reaction–diffusion model. Then, the direct Lyapunov method will be implemented with the aim of identifying certain conditions that guarantee the global asymptotic stability of the steady-state solution. Also, in order to reinforce the credibility of our theoretical framework, several numerical simulations will be provided drawn regarding asymptotic stability. The remainder parts of this article are coordinated in the following manner: In Section 2, we apply a discretization technique to the reaction–diffusion equations to formulate the discrete FHN system. In Section 3, the stability analysis of the discrete FHN system is discussed with the use of its equilibrium points. In Section 4, the global stability of the system at hand is additionally examined. In Section 5, several simulations are performed to validate the conclusions drawn regarding asymptotic stability. At the end of this article, we state the conclusion of our generated results.

2. The discrete FHN model

In this segment, we employ two widely recognized methods to approximate the model under examination. As far as our understanding goes, these discrete models constitute an innovative addition to the current body of literature. In our study, we employed two discretization techniques: the second-order difference approximation and the $L1$ -difference approximation. These methods were chosen due to their established effectiveness and reliability in discretizing reaction–diffusion models, ensuring a balance between accuracy and computational efficiency. The second-order difference approximation is a well-known technique that approximates derivatives by using a central difference scheme. This method provides a higher accuracy compared to first-order differences by considering the function values at adjacent grid points. For a comprehensive understanding of these techniques, we refer readers to the following established literature.^{36,37}

Incorporating these methods into our study provided a robust framework for discretizing the FitzHugh–Nagumo reaction–diffusion model. To accomplish this, we apply the discretization techniques to the following reaction–diffusion equation:

$$\begin{cases} \frac{\partial u}{\partial t} = k\Delta u, & t > 0, \quad \mathfrak{r} \in \Omega, \\ \partial_{\mathfrak{r}} u = 0, & t > 0, \quad \mathfrak{r} \in \partial\Omega, \\ u(0, \mathfrak{r}) = u_0(\mathfrak{r}), & \mathfrak{r} \in \Omega. \end{cases} \tag{1}$$

Utilizing the structure delineated in Eq. (1) and the discretization method expounded in citations,^{38,39} we contemplate the situation where \mathfrak{r} resides within the interval $[0, L]$. This gives rise to the relationship $\mathfrak{r}_{i+1} = \mathfrak{r}_i + k$ for $i = 0, \dots, m$. With the use of the central difference formula to \mathfrak{r} , we derive the estimation for $\frac{\partial^2 u(\mathfrak{r}, t)}{\partial \mathfrak{r}^2}$ as follows:

$$\left\{ \frac{\partial^2 u^n(\mathfrak{r}, t)}{\partial \mathfrak{r}^2} \approx \frac{u^n_{i+1} - 2u^n_i + u^n_{i-1}}{k^2} \right. \tag{2}$$

With the use of the description of the 2nd- and $L1$ - difference approximations for u^n_i as outlined in the Ref. 40, we get

$$\Delta^2 \chi(\ell) = \chi(\ell + 2) - 2\chi(\ell + 1) + \chi(\ell), \quad \ell \in \mathbb{N}. \tag{3}$$

Thus, we can obtain the subsequent approximations:

$$\left\{ \begin{aligned} \frac{\partial^2 u(\mathfrak{r}, t)}{\partial \mathfrak{r}^2} &\approx \frac{\Delta^2 u^n_{i-1}}{k^2}, \\ \frac{\partial u(\mathfrak{r}, t)}{\partial \mathfrak{r}} &\approx \frac{\Delta u^n_i}{h}. \end{aligned} \right. \tag{4}$$

At long last, we reach the following discrete reaction–diffusion equation:

$$\Delta_h u^n_i = \frac{\kappa}{k^2} \Delta^2 u^n_{i-1}, \tag{5}$$

under the following conditions of periodic boundaries:

$$u^n_0 = u^n_m, \quad u^n_1 = u^n_{m+1}. \tag{6}$$

The FHN reaction–diffusion system, as commonly recognized in Ref. 41, was formulated as follows:

$$\begin{cases} \frac{\partial u}{\partial t} = d_1 \Delta u - u^3 + (\tau + 1)u^2 - \tau u - v, & \mathfrak{r} \in \Omega, t > 0, \\ \frac{\partial v}{\partial t} = d_2 \Delta v + \epsilon \{ u^n - \epsilon \tau v \}, & \mathfrak{r} \in \Omega, t > 0, \\ \partial_u = \partial_v = 0, & \mathfrak{r} \in \partial\Omega, t > 0, \\ u(\mathfrak{r}, 0) = u_0(\mathfrak{r}) > 0, \quad v(\mathfrak{r}, 0) = v_0(\mathfrak{r}) > 0, & \mathfrak{r} \in \Omega. \end{cases} \tag{7}$$

Herein, Ω represents a bounded domain in \mathbb{R}^n such that $n = 1$, and it possesses a sufficiently smooth boundary $\partial\Omega$. The operator Δ is defined as $\Delta = \sum_{i=1}^n \frac{\partial^2}{\partial \mathfrak{r}_i^2}$. In this spatially extended system, the variable u signifies the membrane potential, while v characterizes a combination of sodium inactivation and potassium activation at any point $(\mathfrak{r}, t) \in \Omega \times (0, \infty)$. Herein, τ , ϵ and τ are all positive parameters such that τ satisfies the condition $0 < \tau < \frac{1}{2}$, and ϵ being significantly smaller than 1.

The model under investigation in this study is based on the foundational model denoted as (7). Our analysis primarily relies on the discretization method introduced in previous sections. This model, which forms the core of our research, is precisely defined as follows:

$$\begin{cases} \Delta_h u^n_i = \frac{d_1}{k^2} \Delta_{i-1} u^n_i - u_i^{n3} + (\tau + 1)u_i^{n2} - \tau u_i^n - v_i^n, \\ \Delta_h v^n_i = \frac{d_2}{k^2} \Delta_{i-1} v^n_i + \epsilon u_i^n - \epsilon \tau v_i^n, \end{cases} \tag{8}$$

with the periodic boundary conditions

$$\begin{cases} u^n_0 = u^n_m, & u_1 = u_{m+1}, \\ v^n_0 = v^n_m, & v_1 = v_{m+1}, \end{cases} \tag{9}$$

and the initial condition

$$u_i^0 = \mathfrak{f}_1(\mathfrak{r}_i) \geq 0, \quad v_i^0 = \mathfrak{f}_2(\mathfrak{r}_i) \geq 0.$$

3. Local stability

To assess the asymptotic stability of the discrete FHN model mentioned earlier, we focus on the equilibrium points as discussed in Refs. 16, 42. The stability analysis depends on the sign of ϵ , which can be determined using the following expression:

$$\epsilon = (1 - \tau)^2 - \frac{4}{\tau}. \tag{10}$$

Hence, we can consider the three cases listed below:

- In the case where $\epsilon < 0$, the origin $(u_0^*, v_0^*) = (0, 0)$ is the unique fixed point of system (3).
- When $\epsilon = 0$, the origin and $(u_1^*, v_1^*) = \left(-\frac{\tau + 1}{2}, \frac{u_1^*}{\tau}\right)$ are two fixed points for system (3).
- In the case where $\epsilon > 0$, system (3) possesses three fixed points; the origin,

$$(u_2^*, v_2^*) = \left(-\frac{\tau}{2} - \sqrt{\epsilon}, \frac{u_2^*}{\tau}\right) \quad \text{and} \quad (u_3^*, v_3^*) = \left(-\frac{\tau}{2} + \sqrt{\epsilon}, \frac{u_3^*}{\tau}\right).$$

3.1. Local stability of the free diffusions system

The aim of this subsection is to establish the necessary conditions for the local asymptotic stability of the system which has the form

$$\begin{cases} \Delta_h u(t) = -u^3(t) + (\tau + 1)u^2(t) - \tau u(t) - v(t), \\ \Delta_h v(t) = \epsilon u(t) - \epsilon \tau v(t). \end{cases} \tag{11}$$

Accordingly, the following result can be hold.

Theorem 1. System (11) exhibits local asymptotic stability at the equilibrium points under the following conditions:

- When $c = 0$, the equilibrium point (u_0^*, v_0^*) demonstrates local asymptotic stability.
- When $c = 0$, both equilibrium points (u_0^*, v_0^*) and (u_1^*, v_1^*) exhibit local asymptotic stability.
- For $c > 0$, both equilibrium points (u_0^*, v_0^*) and (u_2^*, v_2^*) are locally asymptotically stable. Additionally, the equilibrium point (u_3^*, v_3^*) is stable if the condition

$$\tau \left(\frac{7}{4}\tau + 2 \right) - \sqrt{c}(5\tau + 2) + 3c > 0,$$

is met.

Proof. For the eigenvalues of system (11), the characteristic equation can be found by performing a linear stability analysis about the stable states, i.e.,

$$\mathfrak{J} = \begin{pmatrix} -3u^2 + 2(\tau + 1)u - \tau & -1 \\ \epsilon\tau & -\epsilon \end{pmatrix}. \tag{12}$$

Since system (11) may exhibit multiple equilibria depending on the sign of c , we will individually examine each case.

- By considering that (u_0^*, v_0^*) serves as an equilibrium point, we can then analyze the stability of system (11) irrespective of the sign of c . To do so, we note that $\mathfrak{J}_{(u_0^*, v_0^*)}$ can be represented in the form

$$\mathfrak{J}_{(u_0^*, v_0^*)} = \begin{pmatrix} -\tau & -1 \\ \epsilon\tau & -\epsilon \end{pmatrix}, \tag{13}$$

The characteristic equation for $\mathfrak{J}_{(u_0^*, v_0^*)}$ is then as follows:

$$\mathfrak{A}^2 - \text{tr}(\mathfrak{J}_{(u_0^*, v_0^*)})\mathfrak{A} + \det(\mathfrak{J}_{(u_0^*, v_0^*)}) = 0, \tag{14}$$

where

$$\text{tr}(\mathfrak{J}_{(u_0^*, v_0^*)}) = -\tau - \epsilon \text{ and } \det(\mathfrak{J}_{(u_0^*, v_0^*)}) = \tau\epsilon + \epsilon\tau. \tag{15}$$

This can potentially result in the following discriminant:

$$\mathfrak{D}_{\mathfrak{A}} = \text{tr}^2(\mathfrak{J}_{(u_0^*, v_0^*)}) - 4\det(\mathfrak{J}_{(u_0^*, v_0^*)}) = (\tau + \epsilon)^2 - 4(\tau\epsilon + \epsilon\tau) = (\tau - \epsilon)^2 - 4\epsilon\tau.$$

As $\det(\mathfrak{J}_{(u_0^*, v_0^*)}) > 0$, it is evident that the solutions of (14) depend on the sign of $\text{tr}(\mathfrak{J}_{(u_0^*, v_0^*)})$, and given that $\text{tr}(\mathfrak{J}_{(u_0^*, v_0^*)}) < 0$, it follows that (u_0^*, v_0^*) is asymptotically stable.

- Now, by assuming $c = 0$, we have already established the stability of the origin. Let us now examine the stability of the equilibrium point (u_1^*, v_1^*) . To achieve this goal, we should note that $\mathfrak{J}_{(u_1^*, v_1^*)}$ can be defined by

$$\mathfrak{J}_{(u_1^*, v_1^*)} = \begin{pmatrix} -3\left(\frac{\tau+1}{2}\right)^2 - 2\frac{(\tau+1)^2}{2} - \tau & -1 \\ \epsilon\tau & -\epsilon \end{pmatrix}. \tag{16}$$

Furthermore, we can deduce

$$\text{tr}(\mathfrak{J}_{(u_1^*, v_1^*)}) = \frac{-7(\tau+1)^2}{4} - \tau - \epsilon \text{ and } \det(\mathfrak{J}_{(u_1^*, v_1^*)}) = \left(\frac{7(\tau+1)^2}{4} + \tau\right)\epsilon + \epsilon\tau. \tag{17}$$

This brings us to the discriminant of the eigenvalue problem (14), i.e.,

$$\mathfrak{D}_{\mathfrak{A}} = \frac{7}{2}(\tau+1)^2 \left(\frac{7}{8}(\tau+1)^2 - \epsilon + \tau \right) - 4\epsilon(\tau + \tau) + (\tau + \epsilon)^2.$$

We observe that $\text{tr}(\mathfrak{J}_{(u_1^*, v_1^*)}) < 0$ and $\det(\mathfrak{J}_{(u_1^*, v_1^*)}) > 0$. This assertion along with considering the conclusions drawn regarding the stability of the equilibrium point (u_0^*, v_0^*) confirms that (u_1^*, v_1^*) is asymptotically stable.

- In the final scenario, let us assume that $c > 0$. In this case, the equilibrium point (u_0^*, v_0^*) stills stable. This leads us to analyze the stability of two additional equilibriums.

– Regarding the equilibrium (u_2^*, v_2^*) , we find the following assertion:

$$\mathfrak{J}_{(u_2^*, v_2^*)} = \begin{pmatrix} -3\left(-\frac{\tau}{2} - \sqrt{c}\right)^2 + 2(\tau+1)\left(-\frac{\tau}{2} - \sqrt{c}\right) - \tau & -1 \\ \epsilon\tau & -\epsilon \end{pmatrix}. \tag{18}$$

This results in

$$\text{tr}(\mathfrak{J}_{(u_2^*, v_2^*)}) = -\tau \left(\frac{7}{4}\tau + 2 \right) - \sqrt{c}(5\tau + 2) - 3\tau - \epsilon,$$

and

$$\det(\mathfrak{J}_{(u_2^*, v_2^*)}) = \epsilon \left(\tau \left(\frac{7}{4}\tau + 2 \right) + \sqrt{c}(5\tau + 2) + 3\tau + \tau \right).$$

The discriminant of the eigenvalue problem (14) is given by

$$\mathfrak{D}_{\mathfrak{A}} = \left(-\tau \left(\frac{7}{4}\tau + 2 \right) + \sqrt{c}(-3\tau + 2) - 3\tau + \tau \right)^2 - 4\epsilon\tau.$$

This case is analogous to the situation discussed for the equilibrium point (u_1^*, v_1^*) since $\text{tr}(\mathfrak{J}_{(u_2^*, v_2^*)}) < 0$ and $\det(\mathfrak{J}_{(u_2^*, v_2^*)}) > 0$. Consequently, (u_2^*, v_2^*) is locally asymptotically stable.

– Once more, delving into the stability analysis of the equilibrium (u_3^*, v_3^*) yields the following expressions:

$$\mathfrak{J}_{(u_3^*, v_3^*)} = \begin{pmatrix} -3\left(-\frac{\tau}{2} + \sqrt{c}\right)^2 + 2(\tau+1)\left(-\frac{\tau}{2} + \sqrt{c}\right) - \tau & -1 \\ \epsilon\tau & -\epsilon \end{pmatrix}. \tag{19}$$

Based on the above Jacobian matrix, we can observe

$$\text{tr}(\mathfrak{J}_{(u_3^*, v_3^*)}) = -\tau \left(\frac{7}{4}\tau + 2 \right) + \sqrt{c}(5\tau + 2) - 3\tau - \epsilon,$$

$$\det(\mathfrak{J}_{(u_3^*, v_3^*)}) = \epsilon \left(\tau \left(\frac{7}{4}\tau + 2 \right) - \sqrt{c}(5\tau + 2) + 3\tau + \tau \right).$$

Consequently, we can obtain the following discriminant:

$$\mathfrak{D}_{\mathfrak{A}} = \left(-\tau \left(\frac{7}{4}\tau + 2 \right) + \sqrt{c}(5\tau + 2) - 3\tau + \tau \right)^2 - 4\epsilon\tau. \tag{20}$$

Based on (20), the following cases should be separately analyzed:

- * If $\mathfrak{D}_{\mathfrak{A}} > 0$ and $\det(\mathfrak{J}_{(u_3^*, v_3^*)}) > 0$, then the negativity of the eigenvalues depends on the sign of $\text{tr}(\mathfrak{J}_{(u_3^*, v_3^*)})$. The eigenvalues \mathfrak{A}_1 and \mathfrak{A}_2 are real and negative if and only if $\text{tr}(\mathfrak{J}_{(u_3^*, v_3^*)}) < 0$. This implies that (u_3^*, v_3^*) is asymptotically stable.
- * If $\mathfrak{D}_{\mathfrak{A}} < 0$ and $\det(\mathfrak{J}_{(u_3^*, v_3^*)}) > 0$, then

$$\mathfrak{A}_1 = \frac{\text{tr}(\mathfrak{J}_{(u_3^*, v_3^*)}) - i\sqrt{-\mathfrak{D}_{\mathfrak{A}}}}{2} \text{ and } \mathfrak{A}_2 = \frac{\text{tr}(\mathfrak{J}_{(u_3^*, v_3^*)}) + i\sqrt{-\mathfrak{D}_{\mathfrak{A}}}}{2}. \tag{21}$$

Thus, the solutions can be analyzed on the basis of the sign of $\text{tr}(J_{(u_3^*, v_3^*)})$. In the other words, we can notice that if $\text{tr}(\mathfrak{J}_{(u_3^*, v_3^*)}) > 0$ or $\text{tr}(\mathfrak{J}_{(u_3^*, v_3^*)}) < 0$, then based on the previous analyzed cases, system (11) is asymptotically stable.

- * If $\mathfrak{D}_{\mathfrak{A}} = 0$ and $\det(\mathfrak{J}_{(u_3^*, v_3^*)}) > 0$, then $\text{tr}(\mathfrak{J}_{(u_3^*, v_3^*)})$ could not be zero. The eigenvalues' sign depends on the sign of $\text{tr}(\mathfrak{J}_{(u_3^*, v_3^*)})$. Therefore, (u_3^*, v_3^*) is asymptotically stable if $\text{tr}(\mathfrak{J}_{(u_3^*, v_3^*)}) < 0$, and it is unstable if $\text{tr}(\mathfrak{J}_{(u_3^*, v_3^*)}) > 0$.

Hence, the proof of this result is finished. ■

3.2. Local stability of the diffusion system

In this part, we intend to demonstrate, under specific parameter conditions, that the steady-state (u^*, v^*) can become stable with the

presence of diffusion. For this purpose, we should follow a similar scheme to that used in Ref. 43, starting with the analysis of the eigenvalues of the equation

$$\Delta^2 \kappa_{i-1}^n + \mathfrak{A}_i \kappa_i^n = 0. \tag{22}$$

This analysis considers the following periodic boundary conditions:

$$\kappa_0^n = \kappa_m^n, \quad \kappa_1^n = \kappa_{m+1}^n. \tag{23}$$

To go forward in our examination, we establish the following system:

$$\begin{cases} \Delta_h u_i^n = -\frac{d_1}{k^2} \mathfrak{A}_i u_i^n - u_i^{n3} + (\tau + 1)u_i^{n2} - \tau u_i^n - v_i^n, \\ \Delta_h v_i^n = -\frac{d_2}{k^2} \mathfrak{A}_i v_i^n + \epsilon u_i^n - \epsilon v_i^n. \end{cases} \tag{24}$$

As a result, we can immediately derive the following result.

Theorem 2. System (3) is asymptotically stable if the following conditions are met:

- Consider $\epsilon < 0$ and $(\tau - \epsilon)^2 > 4\epsilon\tau$. System (3) is asymptotically stable at the steady state (u_0^*, v_0^*) if the following conditions are met:

$$\begin{aligned} & -d_1 < d_2 \text{ and } \frac{d_1}{k^2} \mathfrak{A}_i \leq -\tau, \\ & -d_1 > d_2, \frac{d_1}{k^2} \mathfrak{A}_i \leq -\tau, \text{ and} \\ & |\mu_j(\mathfrak{A}_i)| < 1, \quad j = 1, 2. \end{aligned} \tag{25}$$

- If $\epsilon = 0$ and the following condition

$$\frac{7}{2}(\tau + 1)^2 \left(\frac{7}{8}(\tau + 1)^2 - \epsilon + \tau \right) > 4\epsilon(\tau + \tau) - (\tau + \epsilon)^2,$$

is satisfied, then system (3) is asymptotically stable at the steady state (u_1^*, v_1^*) if the following conditions are met:

$$\begin{aligned} & -d_1 < d_2 \text{ and } -\frac{d_1}{k^2} \mathfrak{A}_i \geq \frac{7}{4}(\tau + 1)^2 + \tau, \\ & -d_1 > d_2, -\frac{d_1}{k^2} \mathfrak{A}_i \geq \frac{7}{4}(\tau + 1)^2 + \tau, \text{ and the eigenvalues satisfy condition (27).} \end{aligned}$$

- Considering the case where $\epsilon > 0$ makes us to examine the following two situations:

- If $\left(-\tau \left(\frac{7}{4}\tau + 2\right) - \sqrt{\epsilon(3\tau + 2) - 3\epsilon + \epsilon^2}\right)^2 > 4\epsilon\tau$, then system (3) is asymptotically stable at the steady state (u_2^*, v_2^*) if the following conditions are met:

$$\begin{aligned} & * d_1 < d_2 \text{ and } -\frac{d_1}{k^2} \mathfrak{A}_i \geq \tau \left(\frac{7}{4}\tau + 2\right) + \sqrt{\epsilon(5\tau + 2) + 3\epsilon}. \\ & * d_1 > d_2, -\frac{d_1}{k^2} \mathfrak{A}_i \geq \tau \left(\frac{7}{4}\tau + 2\right) + \sqrt{\epsilon(5\tau + 2) + 3\epsilon}, \text{ and the eigenvalues satisfy condition (27).} \end{aligned}$$

- If $\left(-\tau \left(\frac{7}{4}\tau + 2\right) + \sqrt{\epsilon(3\tau + 2) - 3\epsilon + \epsilon^2}\right)^2 > 4\epsilon\tau$, then system (3) is asymptotically stable at the steady state (u_3^*, v_3^*) if the following conditions are met:

$$\begin{aligned} & * d_1 < d_2 \text{ and } -\frac{d_1}{k^2} \mathfrak{A}_i \geq \tau \left(\frac{7}{4}\tau + 2\right) - \sqrt{\epsilon(5\tau + 2) + 3\epsilon}. \\ & * d_1 > d_2, -\frac{d_1}{k^2} \mathfrak{A}_i \geq \tau \left(\frac{7}{4}\tau + 2\right) - \sqrt{\epsilon(5\tau + 2) + 3\epsilon}, \text{ and the eigenvalues satisfy (27).} \end{aligned}$$

Proof. To examine the local asymptotic stability of the system at hand, we should make a proper linearization. To do so, we should note that if the eigenvalues of the linearized system have negative real parts, then we can conclude that (u^*, v^*) is asymptotically stable. So, we linearize the reaction–diffusion system (24) around the steady state to obtain the following linear system:

$$\mathfrak{J}_i = \begin{pmatrix} -\frac{d_1}{k^2} \mathfrak{A}_i - 3u_i^{n2} + 2(\tau + 1)u_i^n - \tau & -1 \\ \epsilon\tau & -\frac{d_2}{k^2} \mathfrak{A}_i - \epsilon \end{pmatrix}. \tag{26}$$

Herein, we intend to follow the same cases as examined in the free diffusion part as follows:

- We will begin with the origin (u_0^*, v_0^*) . In this case, we have

$$\begin{pmatrix} -\frac{d_1}{k^2} \mathfrak{A}_i - \tau & -1 \\ \epsilon\tau & -\frac{d_2}{k^2} \mathfrak{A}_i - \epsilon \end{pmatrix} = \mathfrak{J}_i(u_0^*, v_0^*) - \lambda(\mathfrak{A}_i)I.$$

This leads to the following eigenvalue equation:

$$\mu^2(\mathfrak{A}_i) - \text{tr}(\mathfrak{J}_i(u_0^*, v_0^*))\mu(\mathfrak{A}_i) + \det(\mathfrak{J}_i(u_0^*, v_0^*)) = 0, \tag{27}$$

where

$$\begin{aligned} \text{tr}(\mathfrak{J}_i(u_0^*, v_0^*)) &= -\left(\frac{d_1}{k^2} + \frac{d_2}{k^2}\right) \mathfrak{A}_i + \text{tr}(\mathfrak{J}(u_0^*, v_0^*)), \\ \det(\mathfrak{J}_i(u_0^*, v_0^*)) &= \frac{d_1}{k^2} \frac{d_2}{k^2} \mathfrak{A}_i^2 + \left(\frac{d_1}{k^2} \epsilon + \frac{d_2}{k^2} \tau\right) \mathfrak{A}_i + \det(\mathfrak{J}(u_0^*, v_0^*)). \end{aligned}$$

Immediately, the discriminant can be expressed as

$$\mathfrak{D}_i = \left(\frac{d_1}{k^2} - \frac{d_2}{k^2}\right)^2 \mathfrak{A}_i^2 + 2\left(\frac{d_1}{k^2} - \frac{d_2}{k^2}\right) (\tau - \epsilon) \mathfrak{A}_i + \Delta_{\mathfrak{A}_i}.$$

The discriminant of \mathfrak{D}_i with respect to \mathfrak{A}_i can be given as

$$\mathfrak{D}_{\mathfrak{A}_i} = \left(\left(\frac{d_1}{k^2} - \frac{d_2}{k^2}\right) (\tau - \epsilon) \mathfrak{A}_i\right)^2 - \left(\frac{d_1}{k^2} - \frac{d_2}{k^2}\right)^2 \mathfrak{A}_i^2 \Delta_{\mathfrak{A}_i} = 4\left(\frac{d_1}{k^2} - \frac{d_2}{k^2}\right)^2 \epsilon\tau.$$

Clearly, since $\mathfrak{D}_{\mathfrak{A}_i} > 0$, we can distinguish between two cases due to the fact that $d_1 \neq d_2$. These cases are as follows:

- If $d_1 < d_2$, then $(\tau - \epsilon)^2 > 4\epsilon\tau$, and both solutions of the equation $\mathfrak{D}_{\mathfrak{A}_i} = 0$ are negative. Thus, $\mathfrak{D}_i > 0$ with significantly noting that these solutions are real. Additionally, $\mu(\mathfrak{A}_i)_1 < 0$. Moreover, if $-\frac{d_1}{k^2} \mathfrak{A}_i \geq \tau$, then $\mu(\mathfrak{A}_i)_2 < 0$. These conditions collectively imply that (u_0^*, v_0^*) is asymptotically stable.
- If $d_1 > d_2$, then we still have $(\tau - \epsilon)^2 > 4\epsilon\tau$, which brings us back to the previous scenario. Once again, if $\frac{d_1}{k^2} \mathfrak{A}_i \geq \tau$, then $\det(\mathfrak{J}_i(u_0^*, v_0^*)) > 0$. Consequently, $\mu_1(\mathfrak{A}_i)$ and $\mu_2(\mathfrak{A}_i)$ are both negative and must satisfy the conditions $|\mu_j(\mathfrak{A}_i)| < 1$.

- Regarding the equilibriums (u_1^*, v_1^*) , (u_2^*, v_2^*) and (u_3^*, v_3^*) , it is worth noting that some straightforward calculations of the Jacobian matrices have led us to the same discriminant $\mathfrak{D}_{\mathfrak{A}_i}$. To avoid redundancy, we have consolidated the results of these calculations in Theorem 2. ■

4. Global stability

The main aim of this part is to show the global asymptotic stability of the constant steady-state solution of the considered system. For this purpose, we state and prove the following result.

Theorem 3. If

$$u^*(\tau + 1 - u^*) < \epsilon, \tag{28}$$

then system (3) achieves consequently global asymptotic stability.

Proof. To illustrate this outcome, the same Lyapunov function is utilized as described in Ref. 44. For see this, we take into consideration the following function:

$$l(z) = z - 1 - \ln(z). \tag{29}$$

The above function exhibits a strict global minimum, namely, $l(1) = 0$. Now, we consider the non-negative function:

$$\mathfrak{L}(t) = \mathfrak{L}_1(t) + \mathfrak{L}_2(t),$$

where

$$\mathfrak{L}_1(t) = \sum_{i=1}^m u^* l\left(\frac{u_i^n}{u^*}\right), \quad \mathfrak{L}_2(t) = \sum_{i=1}^m v^* l\left(\frac{v_i^n}{v^*}\right).$$

Initially, we estimate $\Delta_h \mathbb{L}_1(t)$ as follows:

$$\begin{aligned} \Delta_h \mathbb{L}_1(t) &= \sum_{i=1}^m \Delta_h u^{n*} \Gamma \left(\frac{u_i^n(t)}{u^{n*}} \right), \\ &\leq \sum_{i=1}^m \left(1 - \frac{u^*}{u_i^n} \right) \Delta_h u_i^n, \\ &\leq \sum_{i=1}^m \left(1 - \frac{u^*}{u_i^n} \right) \frac{d_1}{k^2} \Delta^2 u_{i-1}^n - u_i^{n3} + (\tau + 1)u_i^{n2} - \tau u_i^n - v_i^n, \\ &\leq \sum_{i=1}^m \left(1 - \frac{u^*}{u_i^n} \right) u_i^{n3} - (u^*)^3 + (\tau + 1)(u_i^{n2} - (u^*)^2) - \tau(u_i^n - u^*) - v_i^n + v^* \\ &+ \frac{d_1}{k^2} \left(1 - \frac{u^*}{u_i^n} \right) (u_{i+1}^n - 2u_i^n + u_{i-1}^n). \end{aligned}$$

Utilizing (29) yields

$$\begin{aligned} \Delta_h \mathbb{L}_1(t) &\leq \sum_{i=1}^m -(u^*)^3 \left(1 - \frac{u^*}{u_i^n} \right) \left(1 - \frac{u_i^{n3}}{(u^*)^3} \right) \\ &- (u^*)^2(\tau + 1) \left(1 - \frac{u^*}{u_i^n} \right) \left(1 - \frac{u_i^{n2}}{(u^*)^2} \right) \\ &+ \tau u^* \left(1 - \frac{u^*}{u_i^n} \right) \left(1 - \frac{u_i^n}{u^*} \right) + v^* \left(1 - \frac{u^*}{u_i^n} \right) \left(1 - \frac{v_i^n}{v^*} \right) \\ &+ \sum_{i=1}^m \frac{d_1}{k^2} (u_{i+1}^n - 2u_i^n + u_{i-1}^n) - \frac{d_1}{k^2} u^* \left(\frac{u_{i+1}^n}{u_i^n} + \frac{u_{i-1}^n}{u_i^n} - 2 \right), \\ &\leq \sum_{i=1}^m -(u^*)^3 \left(-\Gamma \left(\frac{u_i^n}{u_i^n} \right) - \Gamma \left(\frac{u_i^{n3}}{(u^*)^3} \right) + \Gamma \left(\frac{u_i^{n2}}{(u^*)^2} \right) \right) \\ &- (u^*)^2(\tau + 1) \left(-\Gamma \left(\frac{u_i^n}{u_i^n} \right) - \Gamma \left(\frac{u_i^{n2}}{(u^*)^2} \right) + \Gamma \left(\frac{u_i^n}{u^*} \right) \right) \\ &+ \tau u^* \left(-\Gamma \left(\frac{u_i^n}{u_i^n} \right) - \Gamma \left(\frac{u_i^n}{u^*} \right) \right) \\ &+ v^* \left(-\Gamma \left(\frac{u_i^n}{u_i^n} \right) - \Gamma \left(\frac{v_i^n}{v^*} \right) + \Gamma \left(\frac{u_i^n v_i^n}{u^* v^*} \right) \right) \\ &+ \frac{d_1}{k^2} (u_{m+1}^n - 2u_m^n + u_0^n - u_1^n) - u^* \frac{d_1}{k^2} \left(\frac{u_{i+1}^n}{u_i^n} - 2 + \frac{u_{i-1}^n}{u_i^n} \right). \end{aligned}$$

Once more, we can have

$$\begin{aligned} \Delta_h \mathbb{L}_2(t) &= \sum_{i=1}^m \Delta_h v^* \Gamma \left(\frac{v_i^n}{v^*} \right), \\ &\leq \sum_{i=1}^m \left(1 - \frac{v^*}{v_i^n} \right) \Delta_h v_i^n, \\ &\leq \sum_{i=1}^m \left(1 - \frac{v^*}{v_i^n} \right) \left(\frac{d_2}{k^2} \Delta^2 v_{i-1}^n + \epsilon u_i^n - \epsilon \tau v_i^n \right), \\ &\leq \sum_{i=1}^m \left(1 - \frac{v^*}{v_i^n} \right) (\epsilon(u_i^n - u^*) - \epsilon \tau(v_i^n - v^*)) \\ &+ \frac{d_2}{k^2} \sum_{i=1}^m \left(1 - \frac{v^*}{v_i^n} \right) u_{i+1}^n - 2u_i^n + u_{i-1}^n + o(1), \\ &\leq \sum_{i=1}^m -\epsilon u^* \left(1 - \frac{v^*}{v_i^n} \right) \left(1 - \frac{u_i^n}{u^*} \right) - \epsilon \tau v^* \left(1 - \frac{v^*}{v_i^n} \right) \left(1 - \frac{v_i^n}{v^*} \right) \\ &+ \sum_{i=1}^m \frac{d_2}{k^2} (v_{i+1}^n - 2v_i^n + v_{i-1}^n) - \frac{d_2}{k^2} v^* \left(\frac{v_{i+1}^n}{v_i^n} + \frac{v_{i-1}^n}{v_i^n} - 2 \right), \\ &\leq \sum_{i=1}^m -\epsilon u^* \left(-\Gamma \left(\frac{v_i^n}{v_i^n} \right) - \Gamma \left(\frac{u_i^n}{u^*} \right) + \Gamma \left(\frac{v^* u_i^n}{u^* v_i^n} \right) \right) \\ &- \epsilon \tau v^* \left(-\Gamma \left(\frac{v_i^n}{v_i^n} \right) - \Gamma \left(\frac{v_i^n}{v^*} \right) \right) \\ &+ \frac{d_2}{k^2} (v_{m+1}^n - 2v_m^n + v_0^n - v_1^n) - v^* \frac{d_2}{k^2} \left(\frac{v_{i+1}^n}{v_i^n} - 2 + \frac{v_{i-1}^n}{v_i^n} \right). \end{aligned}$$

In accordance with the Ref. 44, we can obtain

$$\begin{aligned} \frac{u_{i+1}^n}{u_i^n} - 2 + \frac{u_{i-1}^n}{u_i^n} &\geq 0, \\ \frac{v_{i+1}^n}{v_i^n} - 2 + \frac{v_{i-1}^n}{v_i^n} &\geq 0. \end{aligned}$$

In conclusion, we can consequently deduce

$$\begin{aligned} \Delta_h \mathbb{L}(t) &= \Delta_h \mathbb{L}_1(t) + \Delta_h \mathbb{L}_2(t), \\ &\leq \sum_{i=1}^m (u^*)^3 \left(-\Gamma \left(\frac{u_i^n}{u_i^n} \right) - \Gamma \left(\frac{u_i^{n3}}{(u^*)^3} \right) + \Gamma \left(\frac{u_i^{n2}}{(u^*)^2} \right) \right) \\ &+ (u^*)^2(\tau + 1) \left(-\Gamma \left(\frac{u_i^n}{u_i^n} \right) + \Gamma \left(\frac{u_i^{n2}}{(u^*)^2} \right) - \Gamma \left(\frac{u_i^n}{u^*} \right) \right) \\ &+ \tau u^* \left(-\Gamma \left(\frac{u_i^n}{u_i^n} \right) - \Gamma \left(\frac{u_i^n}{u^*} \right) \right) \\ &+ v^* \left(-\Gamma \left(\frac{u_i^n}{u_i^n} \right) - \Gamma \left(\frac{v_i^n}{v^*} \right) + \Gamma \left(\frac{u_i^n v_i^n}{u^* v^*} \right) \right) \\ &+ \epsilon u^* \left(-\Gamma \left(\frac{v_i^n}{v_i^n} \right) + \Gamma \left(\frac{u_i^n}{u^*} \right) - \Gamma \left(\frac{v^* u_i^n}{u^* v_i^n} \right) \right) \\ &+ \epsilon \tau v^* \left(-\Gamma \left(\frac{v_i^n}{v_i^n} \right) - \Gamma \left(\frac{v_i^n}{v^*} \right) \right). \end{aligned}$$

Now, since

$$u^*(\tau + 1 - u^*) < \epsilon, \tag{30}$$

we can draw the conclusion that asserts when $\Delta_h \mathbb{L}(t) \leq 0$ and $\Delta_h \mathbb{L}(t) = 0$, then the only possible equilibrium is $(u_i, v_i) = (0, 0)$. Therefore, under condition (28) stated in Theorem 1, (u^*, v^*) is proven to be globally asymptotically stable. ■

5. Numerical simulations

This section aims to offer a series of numerical simulations to clarify the gained attributes from our theoretical results associated with the stability of the discrete FHN reaction–diffusion system. With the purpose of obtaining a deeper knowledge of the system’s behavior, we investigate how changes in system parameters and order affect its dynamics. To do so, we should mention that the numerical solutions of system (3) has the form

$$\begin{cases} u_i(n\hbar) = \phi_1(x_i) + \hbar \sum_{j=1}^n \left[\frac{u_{i+1}((j-1)\hbar) - 2u_i((j-1)\hbar) + u_{i-1}((j-1)\hbar)}{k^2} \right. \\ \left. - u^3((j-1)\hbar) + (\tau + 1)u^2((j-1)\hbar) - \tau u((j-1)\hbar) - v_i((j-1)\hbar) \right], \\ v_i(n\hbar) = \phi_2(x_i) + \hbar \sum_{j=1}^n \left[\frac{v_{i+1}((j-1)\hbar) - 2v_i((j-1)\hbar) + v_{i-1}((j-1)\hbar)}{k^2} \right. \\ \left. + \epsilon u_i((j-1)\hbar) - \epsilon \tau v_i((j-1)\hbar) \right], \quad 1 \leq i \leq m, \quad n > 0. \end{cases} \tag{31}$$

In this connection, we should concern with the following two cases:

Case 1. To illustrate our point here, we take the values of the parameters as

$$(d_1, d_2, \tau, \epsilon) = (1, 2, 0.2, 0.4), \quad N = 100, \quad \hbar = 0.3, \quad t \in [0, 100], \quad \kappa \in [0, 20], \tag{32}$$

along with the boundary conditions $(u_0, v_0) = (0.1, 0.15)$ and $(u_1, v_1) = (0.1, 0.15)$. We also provide the following initial conditions for the simulation:

$$\begin{cases} \phi_1(x_i) = 1 + \frac{\cos(\pi x_i)}{2}, \\ \phi_2(x_i) = 2.5 + \frac{\cos(\pi x_i)}{2}. \end{cases}$$

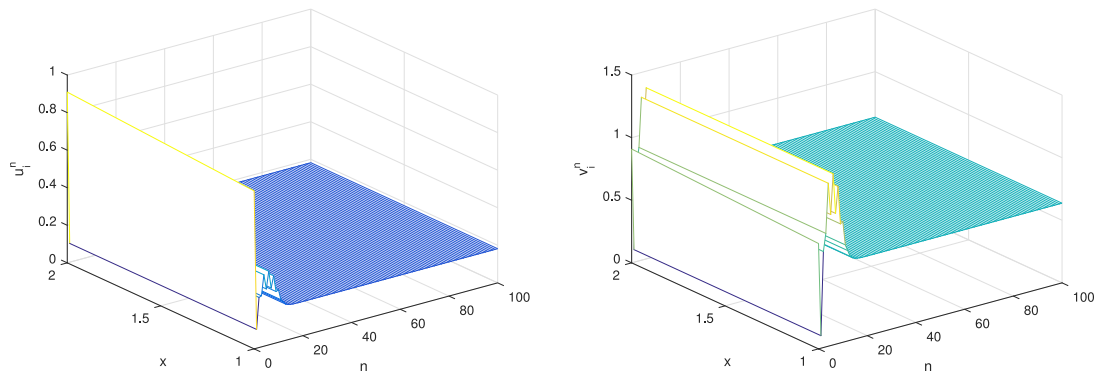


Fig. 1. The one-dimensional concentration profiles of $u_i(t)$ and $v_i(t)$ as solutions to Eq. (8) with the set of parameters (32).

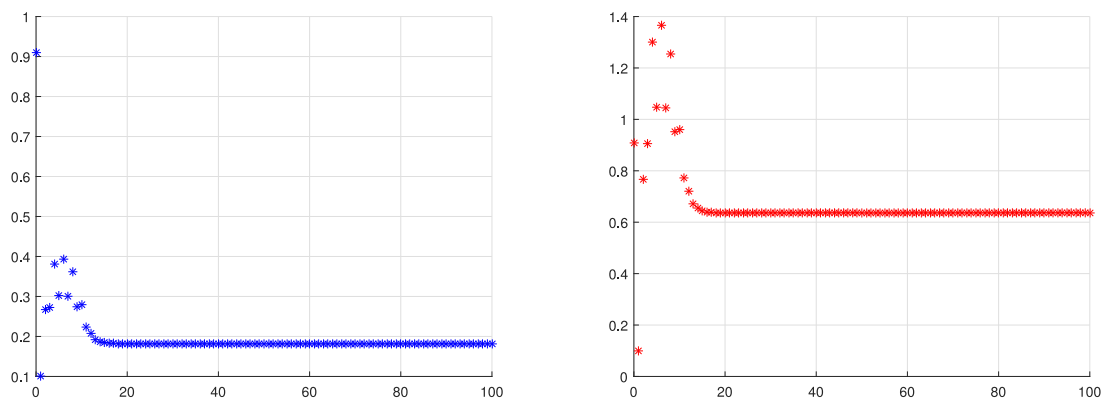


Fig. 2. The time-evolving patterns of $u_i(t)$ and $v_i(t)$ in system (8) with the parameter set (32).

With the help of a prepared MATLAB code, the findings presented in Figs. 1 and 2 visually illustrate the dynamic behavior of system (3). These figures play a crucial role in providing a comprehensive understanding of the system’s stability properties. By observing the model’s behavior over time, it becomes evident that all solutions ultimately converge to a single unique positive equilibrium, which is denoted as $(u^*, v^*) = (0.2, 0.6)$. Furthermore, this equilibrium is characterized as asymptotically stable, indicating that the system will settle into this state regardless of the initial conditions within a certain range.

The graphical representations in Figs. 1 and 2 not only validate the theoretical findings but also offer a deeper insight into the dynamic behavior of the discrete FitzHugh–Nagumo reaction–diffusion system. The time evolution plots in Fig. 1 show that perturbations from the equilibrium decay over time, demonstrating the system’s resilience and its ability to return to a stable state. This is a key aspect of asymptotic stability, indicating that the system can maintain its equilibrium even in the face of small disturbances.

The phase plane analysis in Fig. 2 complements this by illustrating the trajectories in the state space. The spiral and direct paths towards the equilibrium highlight the system’s global stability properties, indicating that the equilibrium point acts as an attractor for all nearby trajectories. This geometric interpretation helps in understanding the comprehensive behavior of the system, providing a visual confirmation of the theoretical stability analysis.

Conclusion

Case 2. Herein, we take into account the parameter values of model (3) as follows:

$$N = 100, (\tau, \epsilon, d_1, d_2) = (0.1, 0.7, 2, 3), \hbar = 0.18, t \in [0, 100], \tau \in [0, 20], \tag{33}$$

along with the boundary conditions $(u_0(t), v_0(t)) = (1, 3)$, $(u_1(t), v_1(t)) = (1, 3)$, and with the initial conditions:

$$\begin{cases} \phi_1(\tau_i) = 1.5 - \cos(\pi\tau_i), \\ \phi_2(\tau_i) = 2 - \cos(\pi\tau_i). \end{cases}$$

Similarly to the aforementioned case, Figs. 3 and 4 effectively illustrate the dynamic behavior of the system and confirm our theoretical findings. These figures play a crucial role in demonstrating the convergence of the model’s solutions to the equilibrium point $(u, v) = (0, 0)$. This equilibrium is shown to be asymptotically stable, reinforcing the validity of our stability analysis.

The graphical representations in Figs. 3 and 4 not only validate the theoretical findings but also offer deeper insights into the dynamic behavior of the system. The time evolution plots in Fig. 3 show that perturbations from the equilibrium decay over time, demonstrating the system’s resilience and its ability to return to a stable state. This is a key aspect of asymptotic

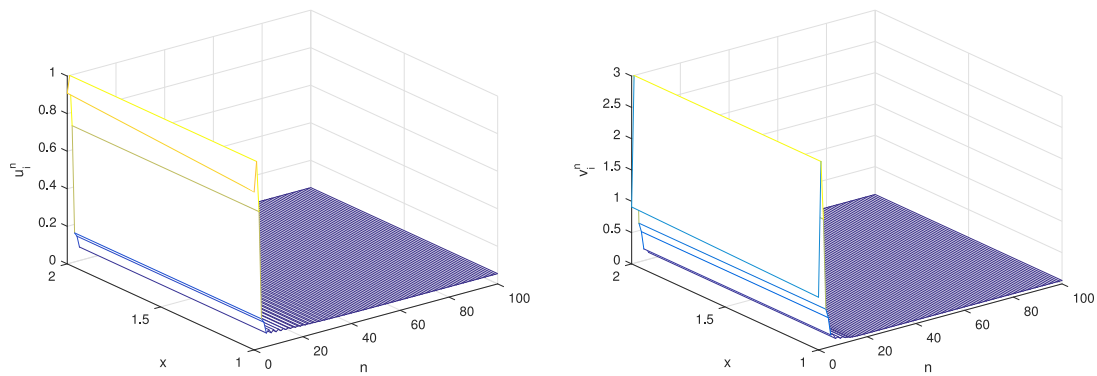


Fig. 3. The one-dimensional concentration profiles of $u_i(t)$ and $v_i(t)$ as solutions to Eq. (8) with the set of parameters (33).

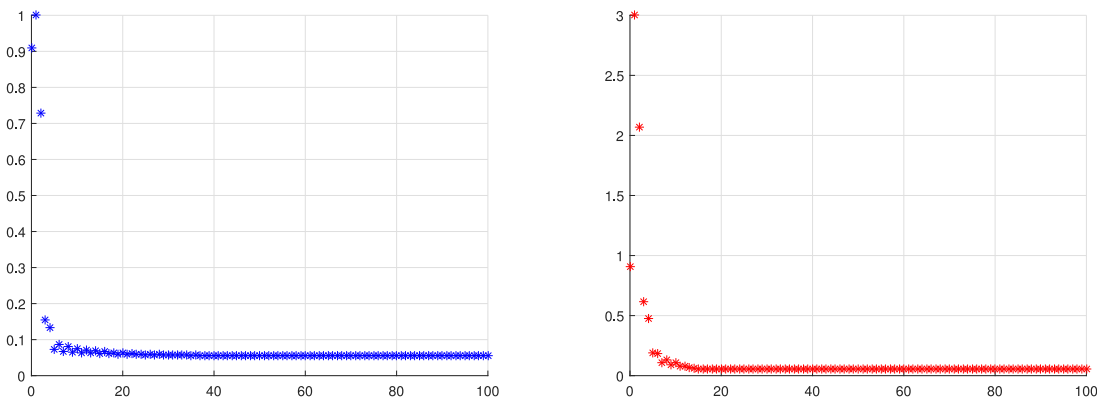


Fig. 4. The time-evolving patterns of $u_i(t)$ and $v_i(t)$ in system (8) with the parameter set (33).

stability, indicating that the system can maintain its equilibrium even in the face of small disturbances.

The phase plane analysis in Fig. 4 complements this by illustrating the trajectories in the state space. The spiral and direct paths towards the equilibrium highlight the system’s global stability properties, indicating that the equilibrium point acts as an attractor for all nearby trajectories. This geometric interpretation helps in understanding the comprehensive behavior of the system, providing a visual confirmation of the theoretical stability analysis.

6. Conclusion

In this paper, we analyzed a discrete FitzHugh–Nagumo reaction–diffusion system by employing the 2nd- and L1-difference approximations. Our investigation focused on the local stability of the equilibrium points, and we derived conditions for global asymptotic stability using the direct Lyapunov method. Through rigorous theoretical analysis and comprehensive numerical simulations, we validated our findings and demonstrated the effectiveness of our approach. Our study makes several significant contributions to the field. Firstly, we successfully applied the 2nd- and L1-difference approximations to discretize the FitzHugh–Nagumo model, providing a robust framework for analyzing discrete reaction–diffusion systems. Secondly, we established criteria for both local and global asymptotic stability of the equilibrium points, contributing to the understanding of the stability properties of discrete nonlinear systems. Thirdly, our numerical simulations corroborate the theoretical results, illustrating the dynamic behavior of the system and reinforcing the validity of the proposed stability conditions. Future research can build upon our findings by exploring the applicability of our methods to higher-dimensional reaction–diffusion systems, which could

provide further insights into complex dynamic behaviors. Additionally, incorporating stochastic variations into the model could enhance the understanding of how random fluctuations influence stability and pattern formation. Applying our theoretical framework to real-world biological or chemical systems could validate the practical utility of our results and potentially uncover new phenomena.

Ethical statement

The authors are accountable for all aspects of the work in ensuring that questions related to the accuracy or integrity of any part of the work are appropriately investigated and resolved.

Declaration of competing interest

The authors declare that they have no known competing financial interests or personal relationships that could have appeared to influence the work reported in this paper.

Data availability

No data was used for the research described in the article.

References

1. FitzHugh R. Impulses and physiological states in theoretical models of nerve membrane. *Biophys J.* 1961;6:445–466.
2. Nagumo J, Arimoto S, Yoshizawa S. An active pulse transmission line simulating nerve axon. *Proc IRE.* 1962;10:2061–2070.
3. Keener JP, Sneyd J. Springer; 1998. *Mathematical Physiology*; vol. 1.
4. Murray JD. *Mathematical biology: I and II, interdisciplinary applied mathematics.* In: *Mathematical Biology.* Springer; 2002.
5. Mann N, Kumar S, Ma WX. Dynamics of analytical solutions and soliton-like profiles for the nonlinear complex-coupled Higgs field equation. *Partial Differ Equ Appl Math.* 2024;10:100733.

6. Kumar S, Mann N. Dynamic study of qualitative analysis, traveling waves, solitons, bifurcation, quasiperiodic, and chaotic behavior of integrable Kuralay equations. *Opt Quantum Electron.* 2024;56:859.
7. Kumar S, Mann N, Kharbanda H, Inc M. Dynamical behavior of analytical soliton solutions, bifurcation analysis, and quasi-periodic solution to the (2+ 1)-dimensional Konopelchenko–Dubrovsky (KD) system. *Anal Math Phys.* 2023;13:40.
8. Bär M, Gottschalk N, Eiswirth M, Ertl G. Spiral waves in a surface reaction: Model calculations. *J Chem Phys.* 1994;100:1202–1214.
9. Barkley D. A model for fast computer simulation of waves in excitable media. *Physica D.* 1991;49:61–70.
10. Karma A. Meandering transition in two-dimensional excitable media. *Phys Rev Lett.* 1990;65:2824.
11. Maz'ya V. *Zur Theorie Sobolewscher Räume, Vol. 38.* Leipzig: Teubner; 1981. In: Teubnertexte Zur Mathematik.
12. Hamadneh T, Hioual A, Saadeh R, et al General methods to synchronize fractional discrete reaction–diffusion systems applied to the glycolysis model. *Fractal Fract.* 2023;7:828.
13. Almatroud OA, Hioual A, Ouannas A, Grassi G. On fractional-order discrete-time reaction diffusion systems. *Mathematics.* 2023;11:2447.
14. Falahah IAbu, Hioual A, Al-Qadri MO, et al Synchronization of fractional partial difference equations via linear methods. *Axioms.* 2023;12:728.
15. Alsayyed O, Hioual A, Gharib GM, et al On stability of a fractional discrete reaction–diffusion epidemic model. *Fractal Fract.* 2023;7:729.
16. Hamadneh T, Hioual A, Alsayyed O, Al-Khassawneh YA, Al-Husban A, Ouannas A. The FitzHugh–Nagumo model described by fractional difference equations: Stability and numerical simulation. *Axioms.* 2023;12:806.
17. Almatroud OA, Hioual A, Ouannas A, Batiha IM. Asymptotic stability results of generalized discrete time reaction diffusion system applied to Lengyel–Epstein and Dagn Harrison models. *Comput Math Appl.* 2024;170:25–32.
18. Hammad MMA, Bendib I, Alshanti WG, et al Fractional-order Degr–Harrison reaction–diffusion model: Finite-time dynamics of stability and synchronization. *Computation.* 2024;12:144.
19. Almatroud OAbdullah, Bendib I, Hioual A, Ouannas A. On stability of a reaction diffusion system described by difference equations. *J Difference Equ Appl.* 2024;30:706–720.
20. Bendib I, Batiha I, Hioual A, Anakira N, Dalah M, Ouannas A. On a new version of Grierer–Meinhardt model using fractional discrete calculus. *Results Nonlinear Anal.* 2024;7:1–15.
21. Krinsky V, Pumir A. Models of defibrillation of cardiac tissue. *Chaos.* 1998;1:188–203.
22. Triki H, Wazwaz AM. On soliton solutions for the Fitzhugh–Nagumo equation with time-dependent coefficients. *Appl Math Model.* 2013;37:3821–3828.
23. Wazwaz AM. *Partial Differential Equations and Solitary Waves Theory.* Springer Science & Business Media; 2010.
24. Shatnawi MT, Khennaoui AA, Ouannas A, et al A multistable discrete memristor and its application to discrete-time FitzHugh–Nagumo model. *Electronics.* 2023;12(13):2929. <http://dx.doi.org/10.3390/electronics12132929>.
25. Shatnawi MT, Abbes A, Ouannas A, Batiha IM. Hidden multistability of fractional discrete non-equilibrium point memristor based map. *Phys Scr.* 2023;98:035213. <http://dx.doi.org/10.1088/1402-4896/acafac>.
26. Hioual A, Oussaeif TE, Ouannas A, Grassi G, Batiha IM, Momani S. New results for the stability of fractional-order discrete-time neural networks. *Alex Eng J.* 2022;61:10359–10369.
27. Hamadneh T, Hioual A, Alsayyed O, Al-Khassawneh YA, Al-Husban A, Ouannas A. Local stability, global stability, and simulations in a fractional discrete glycolysis reaction–diffusion model. *Fractal Fract.* 2023;7(8):587. <http://dx.doi.org/10.3390/fractalfract7080587>.
28. Albadarneh RB, Abbes A, Ouannas A, Batiha IM, Oussaeif TE. On chaos in the fractional-order discrete-time macroeconomic systems. *AIP Conf Proc.* 2023;2849:030014. <http://dx.doi.org/10.1063/5.0162686>, (2023).
29. Batiha IM, Djenina N, Ouannas A. A stabilization of linear incommensurate fractional-order difference systems. *AIP Conf Proc.* 2023;2849:030013. <http://dx.doi.org/10.1063/5.0164866>, (2023).
30. Namjoo M, Zibaei S. Numerical solutions of FitzHugh–Nagumo equation by exact finite-difference and NSFD schemes. *Comput Appl Math.* 2018;37(2):1395–1411.
31. Zhou H, Sheng Z, Yuan G. Physical-bound-preserving finite volume methods for the Nagumo equation on distorted meshes. *Comput Math Appl.* 2019;77(4):1055–1070.
32. Agbavon KM, Appadu AR, Inan B. Comparative study of some numerical methods for the standard FitzHugh–Nagumo equation. In: *Computational Mathematics and Applications.* Springer; 2020:95–127.
33. Agbavon KM, Appadu AR. Construction and analysis of some nonstandard finite difference methods for the FitzHugh–Nagumo equation. *Numer Methods Partial Differ Equ.* 2020;36(5):1145–1169.
34. Inan B, Ali KK, Saha A, Ak T. Analytical and numerical solutions of the Fitzhugh–Nagumo equation and their multistability behavior. *Numer Methods Partial Differ Equ.* 2021;37(1):7–23.
35. Al-Juaifri GA, Harfash AJ. Finite element analysis of nonlinear reaction–diffusion system of Fitzhugh–Nagumo type with Robin boundary conditions. *Math Comput Simulation.* 2023;203:486–517.
36. Thomas JW. Springer Science & Business Media; 2013. *Numerical Partial Differential Equations: Finite Difference Methods*; vol. 22.
37. Diethelm K. *The Analysis of Fractional Differential Equations: An Application-Oriented Exposition Using Differential Operators of Caputo Type.* Springer-Verlag; 2010.
38. Wu GC, Baleanu D, Zeng SD, Deng ZG. Discrete fractional diffusion equation. *Nonlinear Dynam.* 2015;80:281–286.
39. Wu GC, Baleanu D, Xie HP, Zeng SD. Discrete fractional diffusion equation of chaotic order. *Int J Bifurc Chaos.* 2016;26:1650013.
40. Elaydi S. *An Introduction to Difference Equations.* San Antonio, Texas: Springer; 2015.
41. Ouannas A, Mesdoui F, Momani S, Batiha I, Grassi G. Synchronization of FitzHugh–Nagumo reaction–diffusion systems via one-dimensional linear control law. *Arch Contol Sci.* 2021;31.
42. Ringqvist M. On dynamical behaviour of FitzHugh–Nagumo systems. *Research Reports in Mathematics.* 2006;5.
43. Xu L, Zhao LJ, Chang ZX, Feng JT, Zhang G. Turing instability and pattern formation in a semi-discrete Brusselator model. *Modern Phys Lett.* 2013;27:1350006.
44. Yi F, Wei J, Shi J. Global asymptotical behavior of the Lengyel–Epstein reaction–diffusion system. *Appl Math Lett.* 2009;22:52–55.